Distinct element and finite element analyses of underground excavations in jointed rock mass

E. Evgin
Department of Civil Engineering, University of Ottawa, Ottawa, Ontario, Canada
Z. Fu
Department of Civil Engineering, University of Ottawa, Ottawa, Ontario, Canada

ABSTRACT
The deformation and stability of two underground excavations in sedimentary rocks are investigated. Both the finite element and distinct element methods are used to evaluate the differences between the two approaches. This investigation also shows the influence of the orientation of bedding planes on the stability of the tunnels and the size of the excavation damaged zones.

RÉSUMÉ
La déformation et la stabilité de deux excavations sous-sols dans des rochers sédimenteux sont investiguées. Les résultats basés sur la méthode des éléments finis et celle des éléments distincts sont comparées. L'investigation présente l'influence of de la direction des plans de stratification sur la stabilité des tunnels ainsi que sur la taille des zones endommagées.

1 INTRODUCTION

Rock is a common geomaterial in underground engineering practice. Due to the presence of discontinuities such as bedding planes and joints, rock masses behave as anisotropic materials. Closed-form analytical solutions of stresses and displacements around tunnels in elastic anisotropic media are available in the literature (i.e. Hefny and Lo, 1999). However, elastic solutions lack the ability to predict failure. In addition, most commercial finite element and finite difference codes such as Phase2, Plaxis, GeoStudio, SVSolid, and Flac have elasto-plastic anisotropic material models and they eliminate the need for using closed form solutions. On the other hand, the numerical analysis codes mentioned above are based on the continuum idealization and they do not simulate relative movements along discontinuities. In reality, anisotropic rock mass behaviour is controlled by planes of weaknesses. For example, the influence of rock mass anisotropy on the stability of tunnels is shown by Bewick and Kaiser (2009). Discontinuous displacements in a rock mass are best modelled by computer codes such as the distinct element code UDEC.

The literature on the subject of stability and stress-deformation behaviour of tunnels in sedimentary rocks is extensive. Only a few closely related publications are listed here for reference. Lo and Morton (1976) provided theoretical, experimental, and field investigation results related to several tunneling projects in southern Ontario. Lo and Hori (1979) investigated experimentally the deformation and strength properties of sedimentary rocks of five different geological formations in Ontario. Didac et al. (2004) used a "jointed rock model" to simulate anisotropy in their numerical analysis of Envalira Tunnel. Rao et al. (2002) analyzed stresses and deformations in the excavation of Osterfeld Tunnel in 3-D. Compared with in-situ measured deformations at tunnel surface, they found a good agreement between numerical results and in-situ measured values. Kulatilke et al. (2001) used the Universal Distinct Element Code (UDEC) to simulate the strength of jointed block samples. Shen and Barton (1997) also used UDEC to study the excavation disturbed zones around tunnels in jointed rock masses. Tonon (2004) investigated the effects of elastic anisotropy on the plane strain behaviour of a tunnel. In-situ stresses around the Michigan Basin and the geomechanical properties of Paleozoic bedrock formations in southern Ontario are reported by Lam et al. (2007). Perras and Diederichs (2009) conducted a numerical analysis to investigate the influence of the lamination thickness on tunnel response to excavation. Bewick and Kaiser (2009) illustrated the effect of structural features on rock mass disintegration process around deep underground excavations.

In the present study, the effects of excavation of a shallow tunnel and a deep tunnel in cross-anisotropic sedimentary rocks are investigated. First, the finite element code PLAXIS is used to determine the stresses, plastic zones and deformations in the rock mass around the tunnels. Geometric and material nonlinearities are considered. In the second part of the investigation, the distinct element code (UDEC) is utilized to evaluate the effects of discontinuities on rock mass stability around the tunnels. The results of PLAXIS and UDEC are compared to show the similarities and differences in the predictions of the failure zones in sedimentary rocks with various dip angles.

2 SEDIMENTARY ROCKS

Sedimentary rocks are formed from compaction, cementation of sediments or precipitation of crystal aggregates (e.g., shale, siltstone, sandstone, and limestone). In most cases, these types of rocks are cross-anisotropic geomaterials which exhibit isotropic behaviour along bedding planes but anisotropy in orthogonal planes (Lo and Hefny, 1999). Stress and strain relationships of anisotropic sedimentary rocks can be expressed by the following equations. In these equations, the z-axis is in the vertical direction and the x- and y-axes are in horizontal directions.

$$\varepsilon_z = \frac{\sigma_z}{E_v} - \nu_{hv}\frac{\sigma_x}{E_h} - \nu_{hv}\frac{\sigma_y}{E_h} \quad [1]$$

$$\varepsilon_x = \frac{\sigma_x}{E_h} - \nu_h\frac{\sigma_y}{E_h} - \nu_{vh}\frac{\sigma_z}{E_v} \quad [2]$$

$$\varepsilon_y = \frac{\sigma_y}{E_h} - \nu_{vh}\frac{\sigma_z}{E_v} - \nu_h\frac{\sigma_z}{E_h} \quad [3]$$

$$\gamma_{zx} = \frac{\tau_{zx}}{G_{vh}} \quad [4]$$

$$\gamma_{yz} = \frac{\tau_{yz}}{G_{vh}} \quad [5]$$

$$\gamma_{xy} = \frac{2(1+\nu_h)\tau_{xy}}{E_h}\nu_{hv} \quad [6]$$

where E_v = elastic modulus in vertical direction, E_h = elastic modulus in horizontal direction, ν_{vh} = Poisson's ratio for the effect of vertical stress on horizontal strain, ν_{hv} = Poisson's ratio for the effect of horizontal stress on vertical strain, ν_h = Poisson's ratio for the effect of horizontal stress on horizontal strain, and G_{vh} = shear modulus in vertical planes. Elastic material models for cross-anisotropic geomaterials require five independent parameters: E_v, E_h, ν_{vh}, ν_h, and G_{vh}, which are not easy to determine experimentally.

3 TWO-DIMENSIONAL FINITE ELEMENT ANALYSIS USING PLAXIS

The analysis is performed for drained conditions. Plane strain state is assumed and 15-node elements are used for the sedimentary rock.

3.1 Material Model

Parameters required in the present analysis are taken from the publications of Lo and Hefny (1999) and Perras.and Diederichs (2009). The rocks in this area are laminated with a range of bedding thickness from 0.16 to 16 meters. In this study, the lamination thickness (joint spacing) is assumed to be 2 meters. The in-situ stress states, prior to excavation, are established using K_o = 0.5 in the analysis of the shallow tunnel (Note: The measured K_o values in this area are usually much bigger than 0.5) . The behaviour of the sedimentary rock is simulated by the "Jointed Rock Model" in PLAXIS. The elastic modulus of the rock mass in the vertical direction is calculated using Eq. 3.33 given in UDEC User's Guide. The value of the Young's modulus in the horizontal direction is obtained by using the ratio E_h/E_v of 1.7. Anisotropic model parameters are listed in Table 1.

Table 1. Parameters for Jointed Rock Model

Young's Modulus (GPa)	E_v	3.7
	E_h	6.29
Poisson's ratio	γ_{vh}	0.16
	γ_h	0.23
Shear modulus(GPa)	G_{vh}	1.48
Cohesion (GPa)		0.02
Friction angle (degree)		35
Dilatancy angle (degree)		0

3.2 Geometry of 2-D Numerical Model Using PLAXIS

A 10-m-diameter circular tunnel is excavated in the sedimentary rock. A cross section of the tunnel is shown in Figure 1. It is assumed that the tunnel is unsupported.

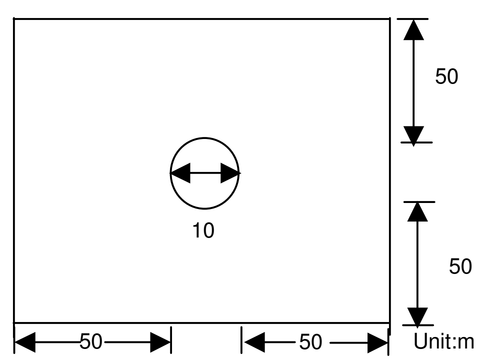

Figure1. Schematics of solution region

Boundary conditions are as follows: the bottom surface of the domain is constrained in all directions and no horizontal movement is allowed at the two vertical sides of the rock mass.

3.3 Results of Numerical Analysis

3.3.1 Stress field around the tunnel

Due to the excavation, the rock mass deforms and the stresses change. It can be seen in Figures 2 and 3 that in Zone 1, horizontal stresses reduce and vertical stresses increase near the springline. In Zone 2, horizontal stresses increase substantially and vertical stresses reduce significantly.

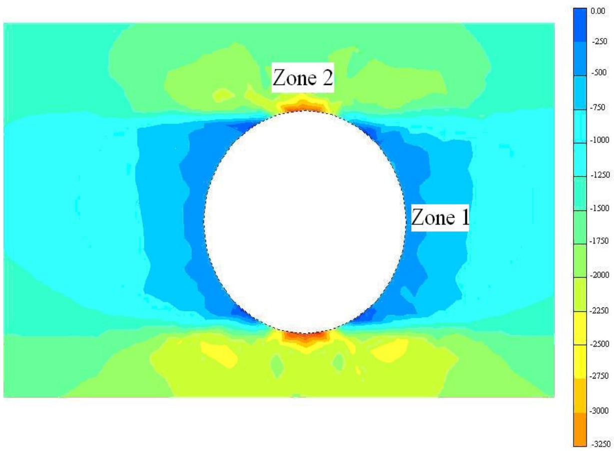

Figure 2 Horizontal stress distributions in rock mass

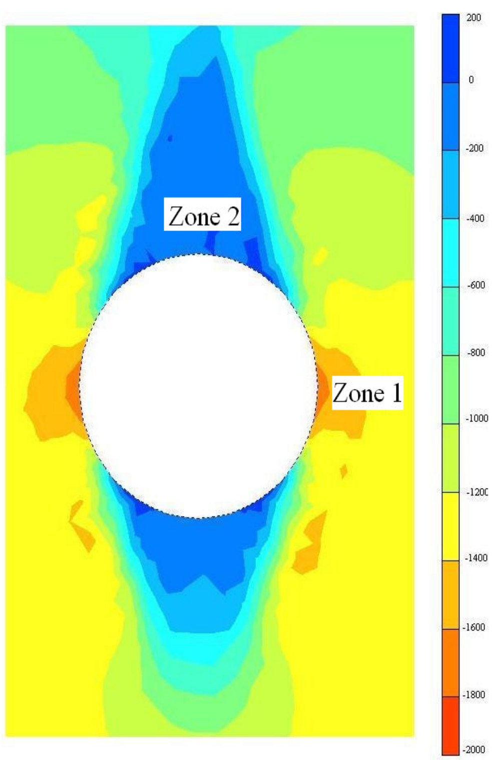

Figure 3 Vertical stress distributions in rock mass

3.3.2 Plastic zones in rock mass

Figure 4 shows the plastic points where most of the stress concentrations and failure take place in the rock mass. In this part of the study, the effects of three bedding plane orientations, i.e, $\Psi=0^{o}$, 45^{o}, and 90^{o} are investigated. The FE results show that plastic zones develop in the same direction as the orientation of the bedding planes during the excavation of the tunnel (Figure 4).

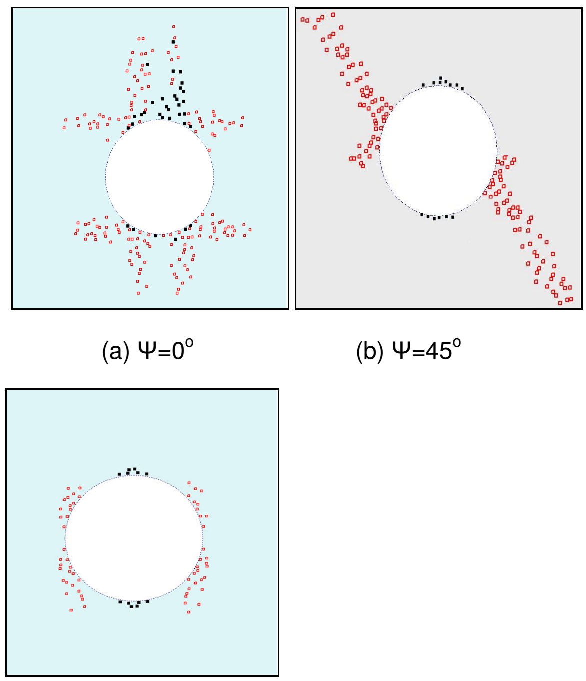

(a) $\Psi=0^{o}$ (b) $\Psi=45^{o}$

(c) $\Psi=90^{o}$

Figure 4 Plastic zones in the rock mass due to excavation

4 DISTINCT ELEMENT ANALYSIS OF TUNNEL EXCAVATION

In the distinct element approach, discontinuous rock masses are represented by an assemblage of discrete blocks with joint sets. There are two types of blocks in UDEC. One is the rigid block which does not change its geometry as a result of applied loading. The other one is deformable blocks which are subdivided into finite difference elements behaving according to a prescribed linear or nonlinear stress-strain constitutive law. In this study, deformable blocks are used. The spacing between the joints is kept constant at 2 metres in all calculations.

The following two types of analyses are performed using UDEC.

4.1 Shallow Tunnel

This is the same problem as analyzed in Section 3. Different joint sets are used in three different analyses to represent the orientation of bedding planes (Ψ) as shown in Figure 5(a, b, c). The material properties of the rock mass are given in Table 2. The Mohr-Coulomb model is used to simulate the behaviour of rock mass. The “Contact-Coulomb Slip Model” is utilized to describe the behaviour of rock joints.

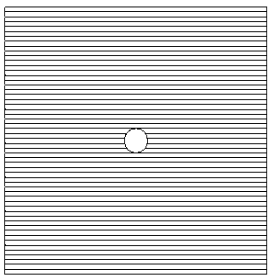

(a) $\Psi=0^{o}$

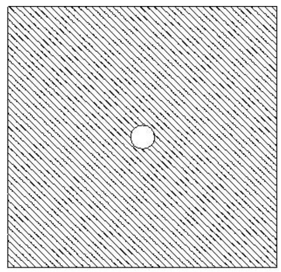

(b) $\Psi=45^{o}$

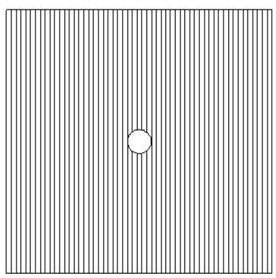

(c) $\Psi= 90^{o}$

Figure 5. Schematic view of 2D models showing the bedding plane orientations

4.2 Numerical Results

Figures 6a, 6b, and 6c show the displacement vectors in the rock mass around the tunnel after excavation for three cases of bedding plane orientations. It can be seen that the orientations of bedding planes have an effect on the displacements in the rock mass. In the case of horizontal bedding in the rock mass, large displacements are in the regions of the crown and invert of the tunnel. When the dip angle is 45^{o}, largest displacements are almost perpendicular to the bedding planes. For the case of 90 degree dip angle the inward displacements of the tunnel walls are almost equal in magnitude all around the circumference of the tunnel.

The shear displacements that are greater than 1 mm along the bedding planes are shown in Figure 7. The shear zones around the tunnel extend about 2-3 times the diameter of the tunnel. The shearing might cause instabilities. Moreover, the flow characteristics of the rock mass in the excavation disturbed zone would be altered. If the purpose of the excavation is to dispose nuclear waste, a detailed investigation of all coupled processes, including the mechanical, thermal, hydrological, and chemical processes, would be necessary. Excessive increase in temperatures, pore water pressures and gas pressures would alter the mechanical and hydraulic characteristics of the rock masses.

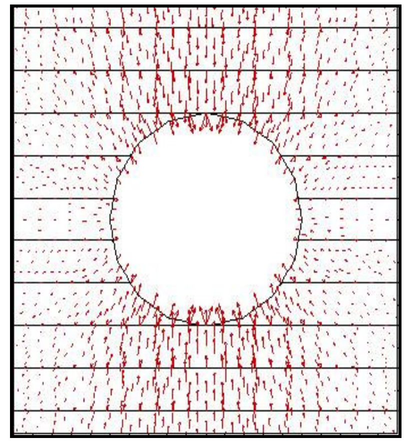

(a) $\Psi=0^{o}$

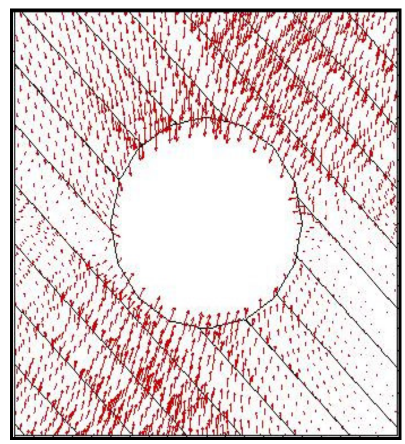

(b) $\Psi=45^{o}$

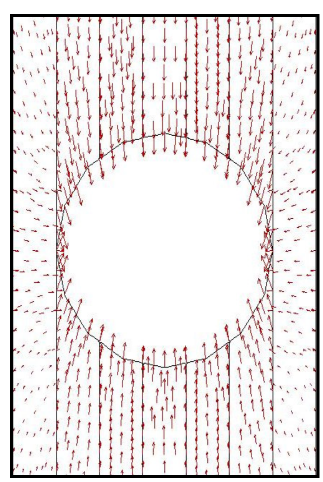

(c) $\Psi=90^{o}$

Figure 6 Displacement vectors in the rock mass around the tunnel due to excavation

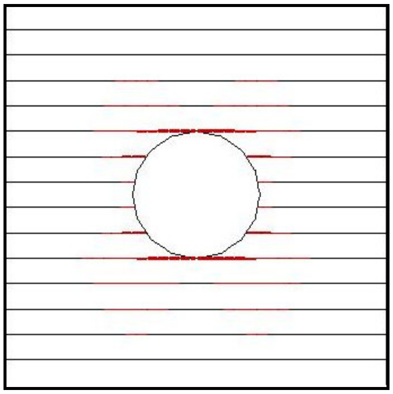

(a) Ψ=0°

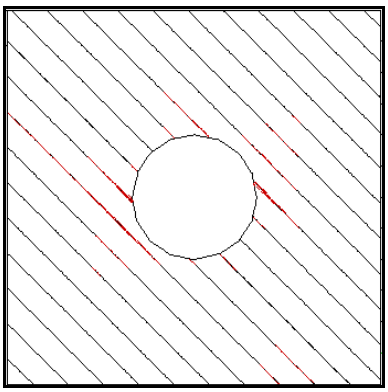

(b) Ψ=45°

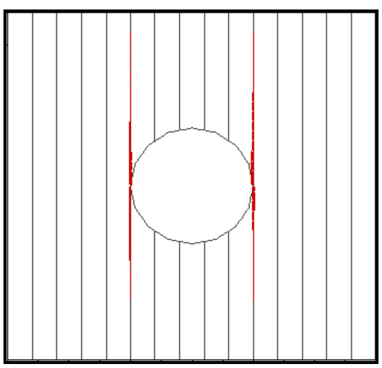

(c) Ψ=90°

Figure7. Shear zones (shear displacement>1mm) around the tunnel as a result of excavation

4.2 Deep Tunnel

A circular tunnel of 16 m diameter is excavated 437 metres below the ground surface. Two cases of dip angles for the bedding planes are considered. In the first case the bedding planes are horizontal. In the second case, the orientation of the bedding planes is chosen 20 degrees measured counter clockwise direction from the horizontal axis. In this problem, K_o was equal to 3. The model parameters are given in Table 2 (see Perras.and Diederichs (2009).

Table 2. Parameters used in UDEC

Bulk modulus (GPa)	K	2.78
Shear modulus (GPa)	G	1.6
Joint normal stiffness (GPa/m)	jkn	25
Joint tangent stiffness (GPa/m)	jks	2.5
Cohesion (MPa)		0.14
Joint friction angle (degree)		25
Tensile strength (MPa)		0.30

UDEC and PLAXIS results for stresses and displacements along LINE 1 and LINE 2 (see Fig, 8) are compared in Figures 9, 10, 11, 12, and 13.

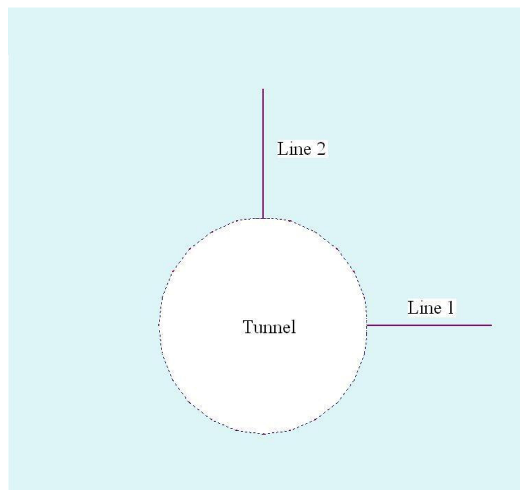

Figure 8. Line 1 and Line 2 are used to plot results

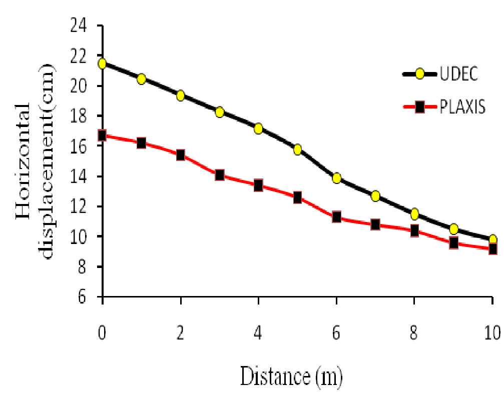

Figure 9. Horizontal displacements along Line 1

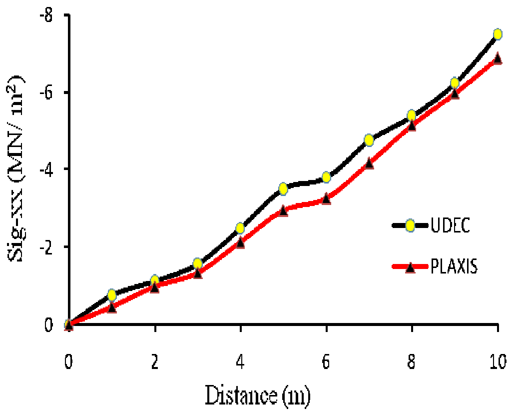

Figure 10. Sig-xx along Line 1

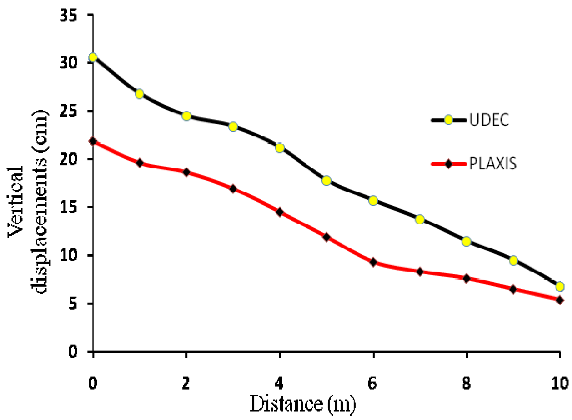

Figure 11. Vertical displacements along Line 2

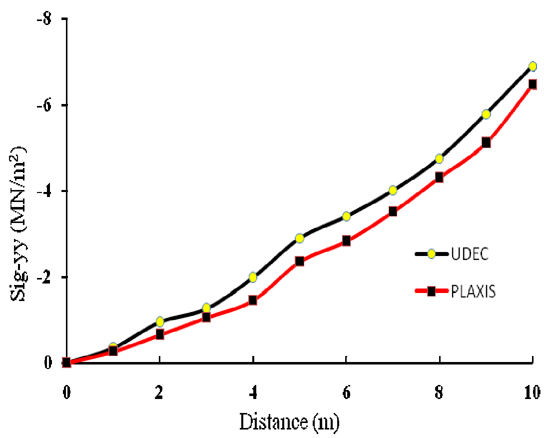

Figure 12 Sig-yy along Line 2

The maximum horizontal and vertical displacements calculated by UDEC are greater than those calculated by PLAXIS as shown in Figures 9 and 11. This is partly due to the ability of UDEC to model large displacements along rock joints. The continuum approach used in PLAXIS is best used for small strain and small deformation. Excessive deformations usually cause numerical problems. Calculated stresses by both methods were very close to each other (Figures 10 and 12).

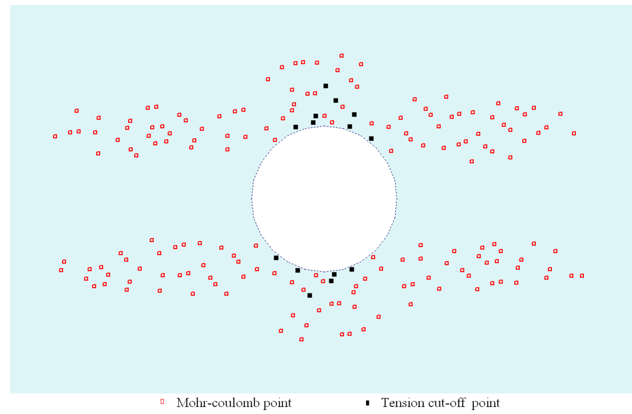

(a) Ψ=0°

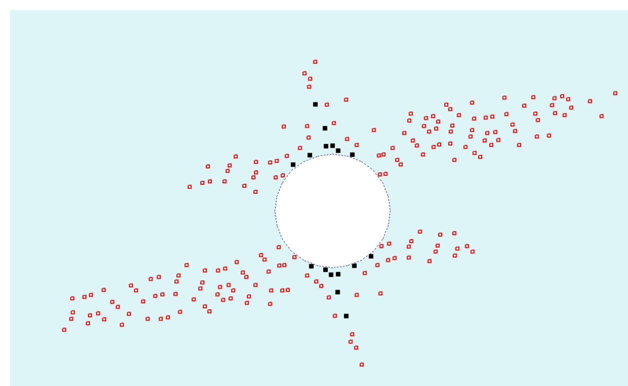

(b) Ψ=20°

Figure 13. Plastic zones in rock mass after excavation (PLAXIS results).

Figures 13a and 13b show the Gauss points where the plastic limit is reached and the failure occurred in the rock mass around the tunnel. These finite element results indicate that plastic zones develop in the same direction as the bedding planes due to the excavation of the tunnel. According to the PLAXIS results, the bands of failed zones extend two to two and a half times the tunnel diameter in each side of the tunnel. Similar observations can be made in UDEC results shown in Fig. 14 for the dip angle equal to zero. In UDEC, the shear failure takes place along two rock joints extending horizontally from the crown and the invert of the tunnel. The difference between the two numerical methods is the thickness of the failure zone. This observation can be useful in the evaluation of the effects of excavation damaged zones on flow patterns in rock masses.

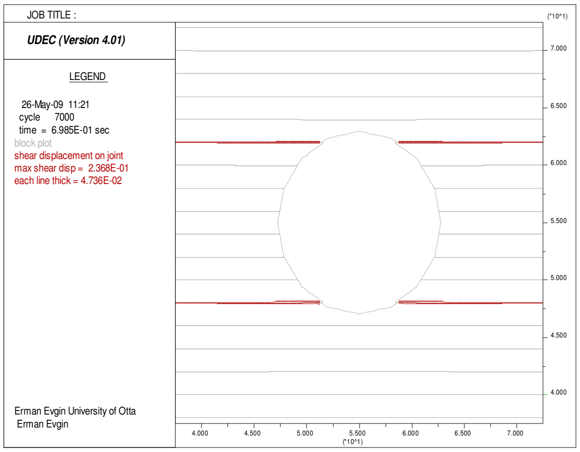

Figure 14. Shear displacements along joints in rock mass due to excavation (UDEC results). Note that only a small portion of the analysis domain is shown for clarity.

The effects of bedding plane orientation on the displacements and stability of the tunnel are shown in Figures 14, 15 and 16. A comparison of these figures suggests two possible stability problems:

1) There is no apparent stability problem when bedding planes are horizontal. However, if the bedding planes make plus or minus 20 degrees with the horizontal plane, instabilities occur.
2) The orientation of bedding planes influences the location of instabilities around the tunnel perimeter. For bedding planes with 20^o angle measured from the horizontal axis in clockwise direction (Fig. 15), some blocks separate from the rock mass at around 1 o'clock and 7~8 o'clock regions. When the bedding planes are oriented at 20 degrees measured from the horizontal axis in counter clockwise direction (Fig. 16), block separation takes place at 4~5 o'clock and ~11 o'clock region. This observation might be useful in the support design.

In all the calculations discussed so far in relation to the deep tunnel, K_o was equal to 3. In order to see the effect of K_o on the stability of the deep tunnel, K_o is reduced to 0.5 in the last run of UDEC. The deformed shape of the tunnel is shown in Fig. 17. There is no obvious instability problem in this case.

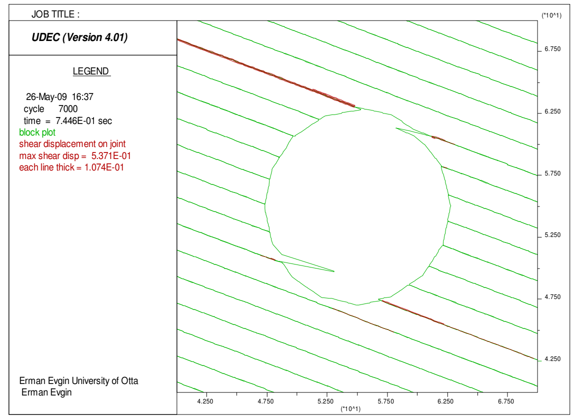

Figure 15. Failure of rock mass at two distinct locations when the dip angle is -20^o (UDEC results)

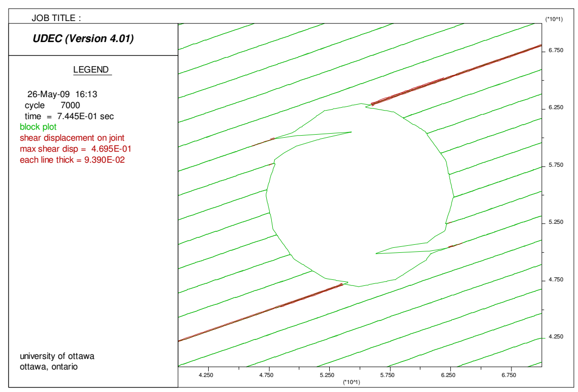

Figure 16. Failure of rock mass at two distinct locations when the dip angle is +20^o (UDEC results)

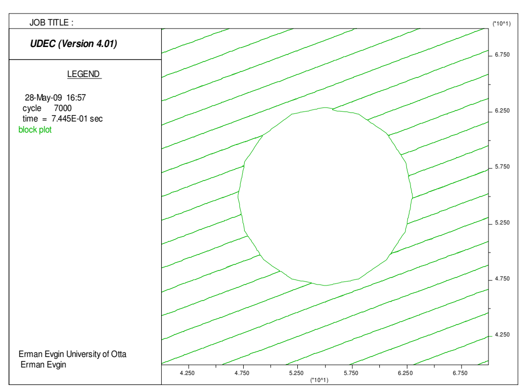

Figure 17. Deformed shape of the tunnel after excavation for K_o=0.5. The orientation of bedding planes is 20^o measured counter clockwise from horizontal axis (UDEC results)

5 CONCLUSIONS

Based on the continuum and discontinuum approaches in the numerical modeling of two tunnels, the following conclusions are drawn:

1) The orientation of bedding planes has a substantial effect on the deformations and stability of the tunnels analyzed in this study.
2) Finite element approach and distinct element approach provide the size of the excavation disturbed zones around the tunnels which are affected by the orientation of the bedding planes. Its effect extends 2-2.5 times the diameter of the tunnel. However, the width of the calculated failure zones is different in the two different approaches.
3) The displacements of the tunnel, calculated by the distinct element approach, are greater than those by the finite element approach in this study.
4) The separation of blocks such as in a rock fall or rotation of rock blocks cannot be modeled by the methods based only on continuum idealization.
5) The effect of bedding plane orientation on the stability of the tunnel is strongly influenced by the value of K_o.

ACKNOWLEDGEMENTS

The financial support for this investigation was provided by the Natural Sciences and Engineering Research Council of Canada.

REFERENCES

Bewick, R.P. and Kaiser, P.K. 2009. Influence of rock mass anisotropy on tunnel stability. ROCKENG09, Proceedings of the 3rd CANUS Rock Mechanics Symposium, Toronto, May 2009, Paper #3995.

Didac, P., Carlos, L., Josep, C., and Père. M. 2004. Numerical analysis of a tunnel in an anisotropy rock mass. Envalira Tunnel *Robert,H., Rafig, A., and Robert C.(Eds):LNES 104*, 153-161.

Itasca Consulting Group, Inc. 2000. *Universal Distinct Element Code*, version 4.0, user's guide.

Kulatilke, P.H.S.W.,Liang J., Gao, H. 2001. Experimental and numerical simulations of jointed rock block strength under uniaxial loading. *Journal of Engineering Mechanics, ASCE,* 127(12), 1240-1247.

Lam, T., Martin, D., and McCreath, D. 2007. Characterising the geomechanics properties of the sedimentary rocks for the DGR excavations. *Canadian Geotechnical Conference*, Ottawa 2007, pp. 636-644.

Lo, K.Y. and Morton, J.D. 1976. Tunnels in bedded rock with high horizontal stresses. *Canadian Geotechnical Journal*, 13:216-230.

Lo, K.Y. and Hori, M. 1979. Deformation and strength properties of some rocks in Southern Ontario. *Canadian Geotechnical Journal*, 16:108-120.

Lo, K.Y. and Hefny,.A.M. 1999. Basic rock mechanics and testing. *Geotechnical and Geoenvironmental Engineering Handbook*. Kluwer Academic Publisher 1999.147-172.

Perras, M.A. and Diederichs, M.S. 2009. Tunnelling in horizontally laminated ground. ROCKENG09, Pro ceedings of the 3rd CANUS Rock Mechanics Symposium, Toronto, May 2009, Paper #3993.

Rao, K.S.,Shrivastava,V.K.,Tiwari,R.P., and Vermeer,P.A. 2002. Excavation—induced stress and deformation analyses of Osterfeld tunnel using Plaxis-3D—*A case study, IGC-2002*, Vol.II, 767-775.

Shen, B. and Barton, N. 1997. The disturbed zone around tunnels in jointed rock masses. Int. J. Rock Mechanics and Mining Sciences. Vol. 34, No. 1, pp. 117-125.

Tonon, F. 2004. Does elastic anisotropy significantly affect a tunnel's plane strain behaviour? *Journal of the Transportation Research Board,* No.1868, 156-168.